

*Invited Paper*

## Hand-held miniature terahertz time-domain attenuated total reflection spectroscopy module

Daniel Molter <sup>1\*</sup>, Garik Torosyan <sup>2</sup>, Jens Klier <sup>1</sup>, Carsten Matheis <sup>1</sup>, Christian Petermann <sup>3</sup>, Stefan Weber <sup>1,4</sup>,  
Frank Ellrich <sup>5</sup>, Joachim Jonuscheit <sup>1</sup>, René Beigang <sup>4</sup>, and Georg von Freymann <sup>1,4</sup>

<sup>1</sup>Fraunhofer Institute for Industrial Mathematics ITWM, Center for Materials Characterization and Testing, 67663  
Kaiserslautern, Germany

<sup>2</sup>Photonik-Zentrum Kaiserslautern e.V., 67663 Kaiserslautern, Germany

<sup>3</sup>TRUMPF Laser GmbH, 78713 Schramberg, Germany

<sup>4</sup>Department of Physics and Research Center OPTIMAS, University of Kaiserslautern, 67663 Kaiserslautern,  
Germany

<sup>5</sup>TH Bingen, University of Applied Sciences, 55411 Bingen

\*<sup>1</sup> Email: daniel.molter@itwm.fraunhofer.de

(Received August 30 2019)

**Abstract:** We present a monolithic silicon module for time-domain attenuated total reflection spectroscopy in the terahertz spectral range. Its volume is less than  $1 \text{ cm}^3$  and is directly merged with the fiber-coupled low temperature grown gallium arsenide emitter and detector antennas. Measurements of liquids, mixtures of liquids, solutions as well as solids are presented. The compactness and direct fiber-coupling of the device makes it flexible for a variety of possible applications.

**Keywords:** Terahertz time-domain spectroscopy, ATR

**doi:** [10.11906/TST.069-076.2019.09.07](https://doi.org/10.11906/TST.069-076.2019.09.07)

### 1. Introduction

Terahertz time-domain spectroscopy (TDS) is a powerful tool for spectroscopic investigations of various types of solids [1] and non-polar liquids. Free-space transmission as well as reflection setups have been reported frequently [2-5]. However, the measurement of opaque media as polar fluids or dissolved substances can hardly be performed in conventional transmission setups. The so-called attenuated total reflection (ATR) spectroscopy uses the evanescent wave at an interface, which reaches into the opaque medium, interacts with it and therefore delivers spectroscopic information afterwards. Up to now, only few simple geometries like prisms [6-11] or waveguides [12] have been reported. Further, free-space propagation of the terahertz radiation before coupling to the ATR modules limits the flexibility of conventional spectroscopy systems. As fiber-coupled terahertz TDS systems grow in importance [13, 14], an ATR spectroscopy system employing fiber-coupling is highly attractive. In this paper we present a flexible, hand-held ATR module of high-resistivity silicon (Si) realized by free-form optics fabrication and merging with the terahertz emitter and detector chips. Measurement results of various liquids, mixtures of

liquids, solutions and solids are presented and demonstrate the usefulness of the introduced device.

## 2. Experimental setup

Photos of the handheld measurement unit and a schematic drawing of the terahertz ATR module are given in Fig. 1.

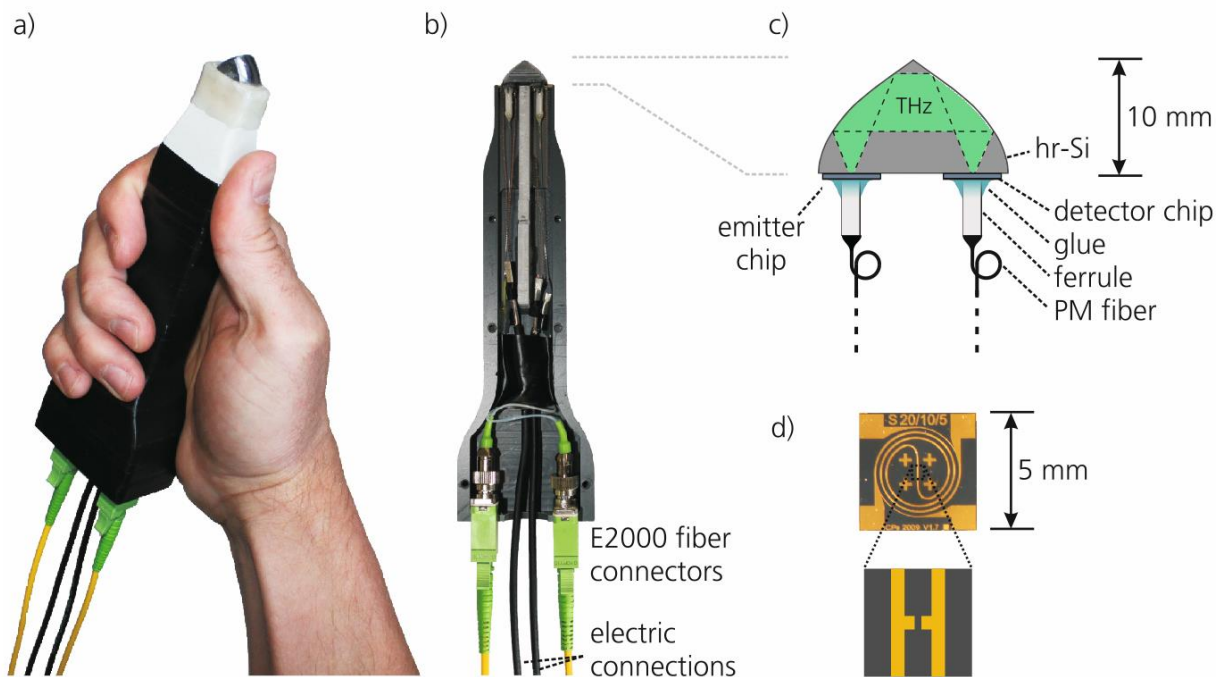


Fig. 1 Photos of the hand-held module (a) and interior (b). Two coaxial cables are used to provide DC voltage to the emitter and to connect the detector antenna to the (external) preamplifier. Two E2000 fiber connectors are used to couple the module via 5 m polarization maintaining fibers to the supply unit. At the monolithic ATR module itself (c), ferrules at the end of the fibers are directly glued to the dipole antenna chips (d). A high-resistivity silicon module, containing two parabolic surfaces, is used for ATR spectroscopy.

The main part of the device is a diamond milled piece of high-resistivity Si featuring two parabolic surfaces, which serve also as the actual sensitive surfaces. The height of the module is 10 mm. The effective focal length of the inverse parabolic mirrors is 5.8 mm. Two low temperature grown gallium arsenide chips ( $5 \times 5 \text{ mm}^2$ ) with dipole metallization (dipole length 20  $\mu\text{m}$ , gap length 5  $\mu\text{m}$ ) serve as emitter and detector and are glued onto the base of the Si module with a center to center distance of 11.6 mm. The metallization striplines feeding the dipoles of the antennas are guided in a spiral to the bond pads. In this way, a miniaturization of the antennas to a small footprint and preventing nearby echoes from the metallization ends is realized at the same time. The terahertz radiation is guided inside the Si in a classical 4f beam path with an overall length of 23.1 mm and free-space propagation is avoided. As the skin depth

of the evanescent wave at the interface is polarization dependent, p-polarization was chosen (dipoles of the antennas on one line). To maintain the advantage and flexibility of integrated emitter and detector chips, fiber ferrules are directly glued to them, providing the pump pulses from the supply unit. By mounting the ATR module on top of a plastic handle with a proper isolation, it can conveniently be dipped into various liquids and powders. As the module is made of Si, it is chemically as well as mechanically very stable.

The scheme of the complete system is shown in Fig. 2, consisting of the already described ATR module and the supply unit. A commercially available fiber laser, delivering pulses of a duration of  $100\text{ fs}$  at an average power of  $100\text{ mW}$  at  $810\text{ nm}$  center wavelength, is used as pump source. A highly efficient transmission grating stretcher is used to prechirp the pulses before being coupled into the polarization maintaining (PM) fibers. After a 50:50 fiber-optic beam splitter, a shaker in one of the arms serves as delay line. It provides the possibility of scanning a maximum delay of  $100\text{ ps}$  at oscillation frequencies up to  $20\text{ Hz}$  (corresponding to  $40\text{ Hz}$  pulse acquisition). Outside the supply unit, which is housed in a 19" rack,  $5\text{ m}$  PM fibers are used to feed the module and provide a high degree of flexibility.

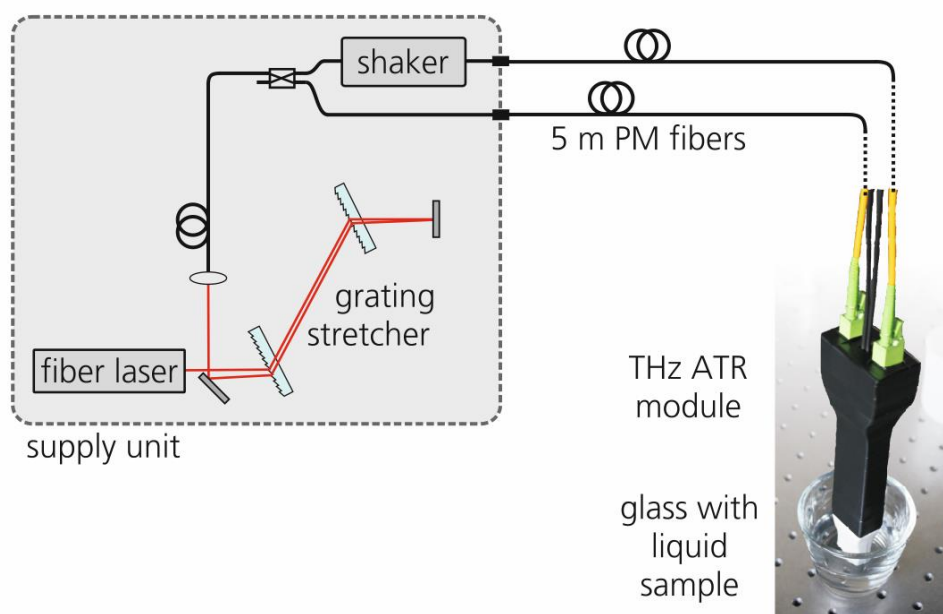


Fig. 2 Scheme of the complete setup. The supply unit, consisting of a fiber laser ( $100\text{ mW}$ ,  $100\text{ fs}$ ,  $810\text{ nm}$ ), a highly efficient transmission grating stretcher, a fiber-optic 50:50 beam splitter and a shaker, is connected to the terahertz ATR module by  $5\text{ m}$  polarization maintaining fibers. The electronics are not shown here.

Data acquisition is realized by using a transimpedance amplifier, a bandpass filter and a data acquisition card. Due to the proximity of the emitter and detector chips, neither optical nor electrical modulation for lock-in technique is used. The emitter chip is biased with a DC voltage of  $50\text{ V}$ .

### 3. Results

Without a sample in contact with the sensitive surfaces, the time trace and its spectrum is as shown in Fig. 3. The main pulse is accompanied by an echo about 10 ps before and one about 10 ps after, whose sources are not yet clear. The data shown is an average of 50 s measurement time. A dynamic range of 1000 and a bandwidth beyond 2 THz is achieved in this measurement.

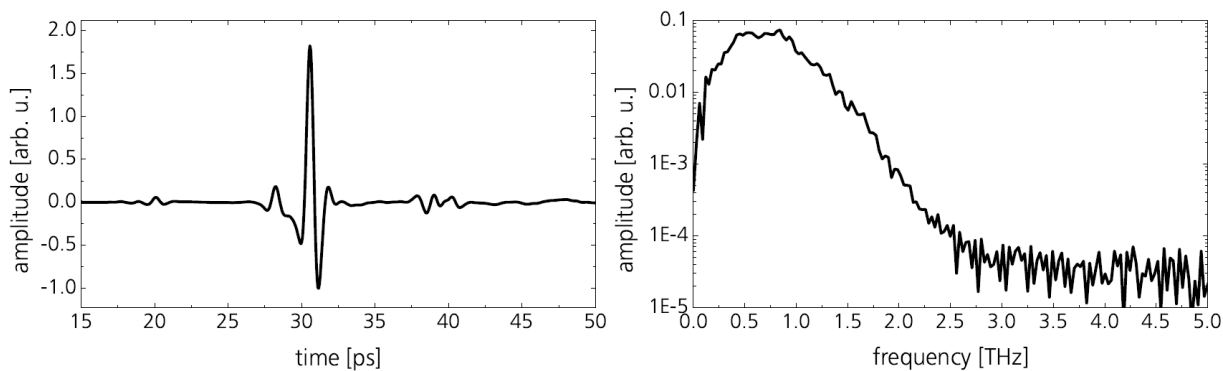


Fig. 3 Time domain signal and FFT of the terahertz ATR module without any sample in contact. A dynamic range of about 1000 and a bandwidth of 2 THz is achieved.

The measurements of four different liquids are shown in Fig. 4. Three types of alcohol (isopropanol, ethanol and acetone) as well as distilled water were measured by simply dipping the ATR module into the liquids. The measurement time for each sample (as well as for those in the following measurements) was 10 seconds. Clearly, water is the most absorbing sample here, while isopropanol has a high amplitude transmission of about 0.8 in average. Even if these liquids do not show sharp spectral fingerprints, differences in the overall trend can be observed. For example, acetone shows a different slope compared to the other samples. The modulation on top of the transmission spectra is expected to be caused by the echo about 2.5 ps before the main pulse in the time trace, which is not consistently changing with the main pulse.

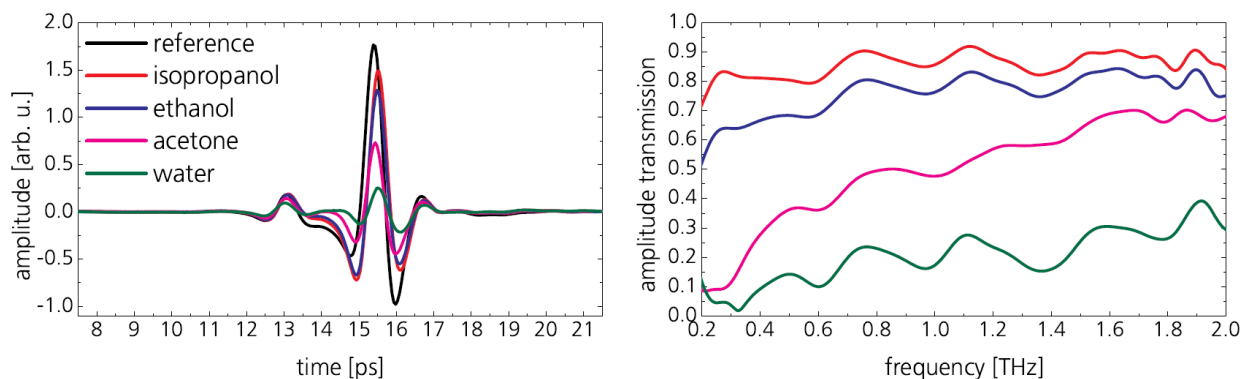


Fig. 4 Time traces and amplitude transmission spectra of isopropanol, ethanol, acetone and (distilled) water. While water is attenuating much, ethanol and isopropanol are highly transparent. This makes them good candidates to be used for solvents in spectroscopic measurements.

The applicability of the ATR module to measure and determine different mixture ratios of fluids by evaluating the change of the amplitude in the time domain is shown in Fig. 5. 60 different mixtures of isopropanol and distilled water as well as 40 mixtures of whiskey and cola were measured and evaluated simply by the amplitude of the pulse in the time domain.

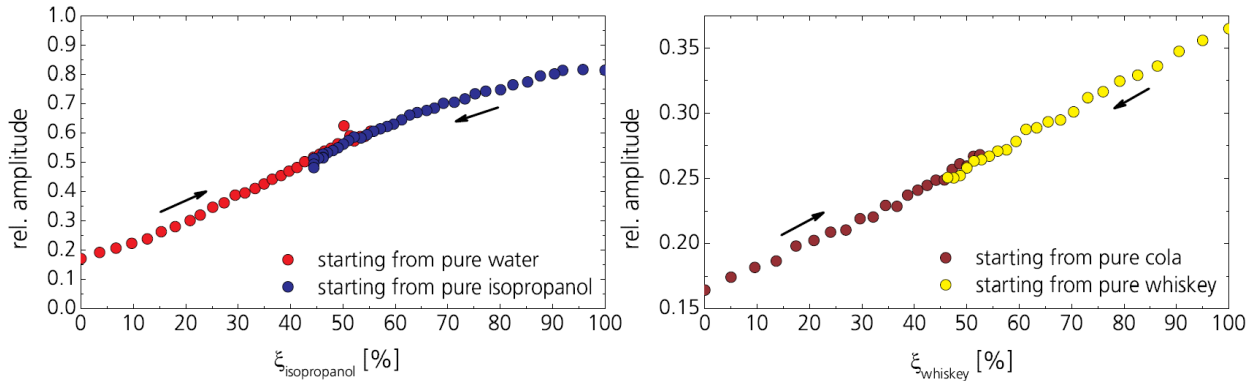


Fig. 5 Evaluation of the relative amplitude (referenced to the signal without sample) for 60 different mixtures of isopropanol and water (left) and 40 different mixtures of whiskey and cola (right). Each plot is combined of two measurement series, starting from the different pure substances. The arrows inserted indicate the measurement sequence.

In both cases a clear dependence on the mixture ratio is observed. While the dependency in the case of whiskey cola mixtures is linear, it is not linear at the isopropanol water mixtures. It is assumed that only in the case of pure substances, as in the case of isopropanol and water, a nonlinear behavior close to the pure substances can be observed. This is also supported by the much higher dynamic in the relative amplitude range for the isopropanol water mixtures (ranging from 0.18 to 0.80) compared to the whiskey cola mixtures (ranging from 0.17 to 0.37).

A measurement of the relative change in the amplitude in dependency on the frequency and the glucose concentration in water is shown in Fig. 6.

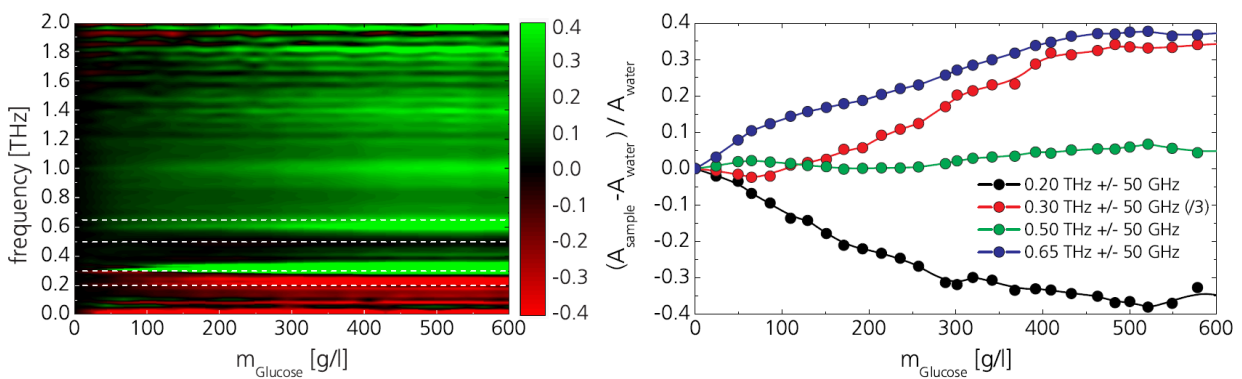


Fig. 6 Left: Frequency and glucose concentration dependent relative change in the amplitude  $(A_{\text{sample}} - A_{\text{water}}) / A_{\text{water}}$ . Right: Plot for four characteristic frequencies indicated with dashed lines in the intensity plot (left). Connecting lines are guide for the eye.

For frequencies below approx.  $0.28 \text{ THz}$ , bulk water is less absorbing than the glucose solution, resulting in a decrease of the amplitude with increasing concentration. At  $0.3 \text{ THz}$ , three different regions can be observed. Up to  $100 \text{ g/l}$ , the amplitude is decreasing, from  $100 \text{ g/l}$  to the specified saturation concentration of about  $470 \text{ g/l}$  it is increasing and above it is saturating. A possible explanation of the behavior up to  $100 \text{ g/l}$  could be the formation of hydration shells [15], which have a higher absorption at this specific frequency. After a certain concentration (here  $100 \text{ g/l}$ ), the overall occupied volume of the hydration shells saturates and the lower absorption of the glucose beats the characteristic of the hydration shells. This explanation suggests, that at a frequency of  $0.65 \text{ THz}$ , the hydration shells are less absorptive than the glucose molecules resulting in a higher slope for concentrations below  $100 \text{ g/l}$  than above. At this frequency, the saturation concentration can nicely be confirmed.

To test the spectroscopic applicability of the ATR module, powders of para-aminobenzoic acid (PABA), lactose and tartaric acid were each mixed with ethanol, brought onto the sensitive surfaces and measured after drying out. With this procedure a good contact to the Si surface is ensured. The measurement results and a comparison to conventional transmission measurements is shown in Fig. 7.

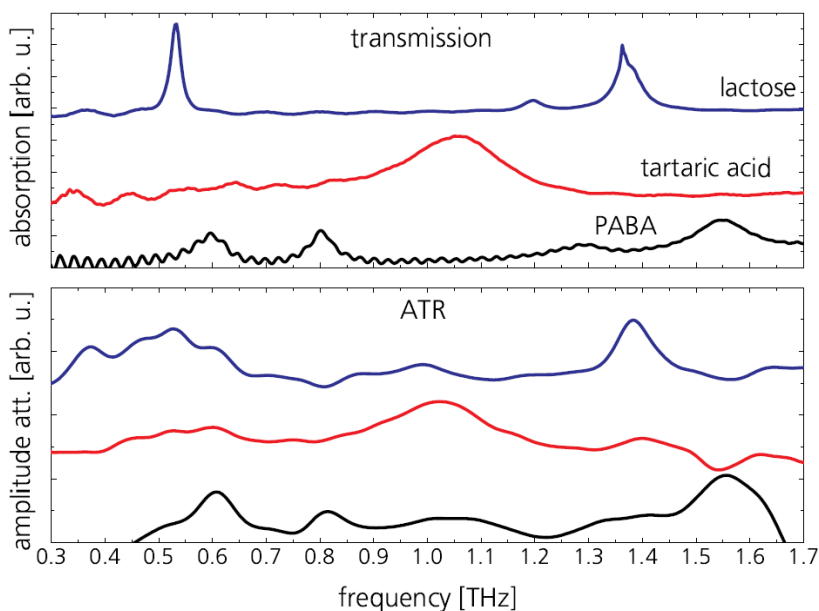


Fig. 7 Comparison of absorption spectra measured with conventional transmission terahertz TDS (top) and with the ATR module (bottom). Samples of para-aminobenzoic acid (PABA), lactose and tartaric acid were mixed with ethanol and applied to the sensitive surfaces of the ATR module. The measurement was performed after the evaporation of the ethanol. (Baselines are vertically shifted for clarity. Only a qualitative comparison is intended here.

The transmission measurements were performed with pressed pellets of the same substances. In all three cases, characteristic peaks in the absorption spectra can be found, even if the baselines are not smooth. This proves the applicability of the miniature ATR device to spectroscopic

measurement tasks.

#### 4. Conclusion

In summary we have developed a fiber-coupled, hand-held terahertz ATR module based on a high-resistivity Si body. Free-form optics fabrication was used to realize a classical 4f beam path inside the material with two off-axis parabolic surfaces, which act as inverse mirrors and therefore are the sensitive interfaces of the module. The fiber-coupled emitter and detector chips were directly glued to the base of the ATR body to maintain the flexibility of the device. With this design no free-space propagation of either the pump or the terahertz radiation is used. Various measurements of liquids, mixtures of liquids, solvents as well as solids were presented and demonstrate the usefulness of the device. Future improvements by increasing the interaction volume by tailoring the geometry of the Si module is feasible. As the supply unit is identical to the one used in [16], increase of the measurement speed up to pulse acquisition rates of about 200 Hz is straightforward. The transfer of this concept to terahertz TDS systems using telecom wavelength is conceivable by using already established photoconductive switches designed for this wavelength range [17]. The further increase of measurement speed can be achieved by using modern delay-line-free terahertz sampling concepts [18, 19]. We already have fabricated a module based on an ellipsoidal surface, which we consider to implement and test as well. More complex geometries beyond parabolic and ellipsoidal surfaces as well as increase of the number of interfaces is conceivable.

#### Acknowledgements

We gratefully acknowledge the kind support of Matthias Heyden in interpretation of the measurement results shown in Fig. 6.

#### References

- [1] D. Grischkowsky, S. Keiding, M. v. Exter, et al. "Far-infrared time-domain spectroscopy with terahertz beams of dielectrics and semiconductors". *J. Opt. Soc. Am. B* 7, 2006–2015 (1990).
- [2] A. Nahata, A. S. Weling, and T. F. Heinz. "A wideband coherent terahertz spectroscopy system using optical rectification and electro-optic sampling". *Appl. Phys. Lett.* 69, 2321–2323 (1996).
- [3] P. U. Jepsen and B. M. Fischer. "Dynamic range in terahertz time-domain transmission and reflection spectroscopy". *Opt. Lett.* 30, 29–31 (2005).
- [4] S. Nashima, O. Morikawa, K. Takata, et al. "Measurement of optical properties of highly doped silicon by terahertz time domain reflection spectroscopy". *Appl. Phys. Lett.* 79, 3923–3925 (2001).

- [5] H.-B. Liu, Y. Chen, G. J. Bastiaans, et al. "Detection and identification of explosive RDX by THz diffuse reflection spectroscopy". *Opt. Express* 14, 415–423 (2006).
- [6] C. Rau, G. Torosyan, and R. Beigang. "Prism coupled terahertz waveguide sensor". *Appl. Phys. Lett.* 86, 211119 (2005).
- [7] D. A. Newnham and P. F. Taday. "Pulsed Terahertz Attenuated Total Reflection Spectroscopy". *Appl. Spectrosc.* 62, 394–398 (2008).
- [8] H. Hirori, K. Yamashita, M. Nagai, et al. "Attenuated Total Reflection Spectroscopy in Time Domain Using Terahertz Coherent Pulses". *Jpn. J. Appl. Phys.* 43, L1287–L1289 (2004).
- [9] Y. Zou, Q. Liu, X. Yang, et al. "Label-free monitoring of cell death induced by oxidative stress in living human cells using terahertz ATR spectroscopy". *Biomed. Opt. Express* 9, 14-24 (2018).
- [10] K. Takeya, K. Muto, Y. Ishihara, et al. "Monitoring Theophylline Concentrations in Saline Using Terahertz ATR Spectroscopy". *Appl. Sci.* 6, 72 (2016).
- [11] A. Soltani, S. F. Busch, P. Plew, et al. "THz ATR Spectroscopy for Inline Monitoring of Highly Absorbing Liquids". *J. Infrared Milli. Terahz. Waves* (2016).
- [12] L. Cheng, S. Hayashi, A. Dobroiu, et al. "Terahertz-wave absorption in liquids measured using the evanescent field of a silicon waveguide". *Appl. Phys. Lett.* 92, 181104 (2008).
- [13] F. Ellrich, T. Weinland, D. Molter, et al. "Compact fiber-coupled terahertz spectroscopy system pumped at 800 nm wavelength". *Rev. Sci. Instrum.* 82, 053102 (2011).
- [14] R. J. B. Dietz, B. Globisch, H. Roehle, et al. "Fiber coupled terahertz time domain spectroscopy system based on InGaAs/InAlAs photoconductors with 100 dB dynamic range". 40th International Conference on Infrared, Millimeter, and Terahertz waves (IRMMW-THz), Hong Kong, pp. 1-2 (2015).
- [15] M. Heyden, E. Bründermann, U. Heugen, et al. "Long-Range Influence of Carbohydrates on the Solvation Dynamics of Waters – Answers from Terahertz Absorption Measurements and Molecular Modeling Simulations". *J. Am. Chem. Soc.* 130, 5773-5779 (2008).
- [16] D. Molter, F. Ellrich, T. Weinland, et al. "High-speed terahertz time-domain spectroscopy of cyclotron resonance in pulsed magnetic field". *Opt. Express* 18, 26163–26168 (2010).
- [17] R. B. Kohlhaas, R. J. B. Dietz, S. Breuer, et al. "Improving the dynamic range of InGaAs-based THz detectors by localized beryllium doping: up to 70 dB at 3 THz". *Opt. Lett.* 43, 5423-5426 (2018).
- [18] R. J. B. Dietz, N. Vieweg, T. Puppe, et al. "All fiber-coupled THz-TDS system with kHz measurement rate based on electronically controlled optical sampling". *Opt. Lett.* 39, 6482-6485 (2014).
- [19] M. Kolano, B. Gräf, S. Weber, et al. "Single-laser polarization-controlled optical sampling system for THz-TDS". *Opt. Lett.* 43, 1351-1354 (2018).